

Edge states and spin-valley edge photocurrent in transition metal dichalcogenide monolayers

V. V. Enaldiev*

Kotel'nikov Institute of Radio-engineering and Electronics, Russian Academy of Sciences, 11-7 Mokhovaya Street, Moscow 125009, Russia

(Received 2 November 2017; published 21 December 2017)

We develop an analytical theory for edge states in monolayers of transition metal dichalcogenides based on a general boundary condition for a two-band **kp** Hamiltonian in the case of uncoupled valleys. Taking into account *edge* spin-orbit interaction, we reveal that edge states, in general, have linear dispersion that is determined by three real phenomenological parameters in the boundary condition. In the absence of the edge spin-orbit interaction, edge states are described by a single real parameter whose sign determines whether their spectra intersect the bulk gap or not. In the former case we show that illumination by circularly polarized light results in spin- and valley-polarized photocurrent along the edge. Flow direction and spin and valley polarization of the edge photocurrent are determined by the direction of circular polarization of the illuminated light.

DOI: [10.1103/PhysRevB.96.235429](https://doi.org/10.1103/PhysRevB.96.235429)

I. INTRODUCTION

The optical properties of monolayer crystals of transition metal dichalcogenides (TMDs; such as MoS₂, MoSe₂, MoTe₂, WS₂, and WSe₂) have recently attracted considerable interest due to possible optoelectronic applications [1,2]. This is due to the direct band gap of the TMD monolayers whose value corresponds to the visible and infrared light frequencies [3]. The optical response of the bulk materials at the absorption edge is dominated by excitons [4]. However, recent experiments on second-harmonic generation at subband gap frequencies [5], scanning tunneling microscopy and spectroscopy [6,7], and microwave impedance microscopy [8] in MoS₂ monolayers have also exhibited edge state (ES) signs.

From a theoretical point of view properties of ESs in atomically thin MoS₂ have been extensively studied in the frameworks of density-functional theory [7,9–13] and tight-binding approximation [14,15]. However, a description of the ESs in the TMD monolayers within the **kp** approach allows one to describe the ESs without going into the details of the edge microscopic structure and to take into account effects of external fields. This enables one to construct an analytic theory for the ESs in the whole class of materials in a unified way. Such a general theory relies on a boundary condition (BC) that describes the edge structure by means of several phenomenological parameters. The values of these parameters can be obtained by fitting with experimental data or other calculations based on density-functional or tight-binding approximations. The authors of Ref. [16] derived a general boundary condition taking into account valley coupling at the edge and neglecting spin-orbit interaction at the edge, which may, in general, exist (see Ref. [17] and references therein). Recently, ES spectra in the TMD monolayer nanoribbon [18] and optical absorption in TMD nanoflakes involving transitions between the bulk and edge states [19] have been studied using the **kp** approximation. However, these studies were restricted by some specific values of the phenomenological boundary parameters.

The aim of this paper is twofold. First, we develop an analytical theory for the ESs in the TMD monolayers in the **kp** approach taking into account *edge* spin-orbit interaction

(ESOI) in the case of uncoupled valleys. Second, we consider optoelectronic properties of the ESs and demonstrate the emergence of spin- and valley-polarized edge photocurrents due to illumination of the monolayer by circularly polarized light. The origin of the effect concerns selection rules for optical transitions from bulk states to edge states caused by circularly polarized light in the two valleys. The selection rules are essentially different from those for interband optical transitions in the bulk that give rise, for example, to the valley Hall effect [20]. This paper is organized as follows: in Sec. II we derive a general boundary condition and resulting ES spectra for the two-band continuum model, and Sec. III is devoted to the derivation of the edge photocurrent.

II. EDGE STATES IN THE TWO-BAND **kp** APPROXIMATION

In the TMD monolayers conduction and valence band edges are located in the *K* and *K'* valleys of the honeycomb lattice Brillouin zone. Within a two-band **kp** approach, the dynamics of electrons in the *K* (*K'*) valley is described by the Hamiltonian [3,21]

$$H_{\tau} = \begin{pmatrix} m + \tau \Delta_c & vp_{-\tau} & 0 & 0 \\ vp_{+\tau} & -m + \tau \Delta_v & 0 & 0 \\ 0 & 0 & m - \tau \Delta_c & vp_{-\tau} \\ 0 & 0 & vp_{+\tau} & -m - \tau \Delta_v \end{pmatrix} \quad (1)$$

where $2m$ is the band gap without spin splitting, $2\Delta_{c,v}$ are the values of spin splitting in the conduction and valence bands, respectively, the index $\tau = +1$ (-1) denotes the *K* (*K'*) valley, $p_{\pm,\tau} = \tau p_x \pm ip_y$ (p_x, p_y are components of in-plane momentum), and v is the velocity matrix element between the band extrema. The Hamiltonian H_{τ} (1) possesses a diagonal form in the spin subspace, with the upper left (lower right) block acting on two-component wave functions of spin-up (spin-down) states. To describe the edge of the TMD monolayer one should supplement the Hamiltonian with a BC for envelope wave functions. In the present work we consider a translation-invariant edge for which projections of the valley centers onto the edge direction are very distant from each other

*vova.enaldiev@gmail.com

(like at zigzag or reconstructed zigzag edges). Therefore, we neglect the valley coupling at the edge.

However, even at the translation-invariant edge, additional ESOI can mix the spins. Let us derive the most general BC that describes this entanglement in our model. Since H_τ (1) is first order in momentum, a general BC has the form of a linear combination of two-component wave functions $\Psi_\tau^{\uparrow(\downarrow)} = (\psi_{c,\tau}^{\uparrow(\downarrow)}, \psi_{v,\tau}^{\uparrow(\downarrow)})^T$ belonging to spin-up (spin-down) states:

$$[\Psi_\tau^\uparrow - M_\tau \Psi_\tau^\downarrow]_{\text{edge}} = 0, \quad (2)$$

where M_τ is the second-order square matrix consisting of phenomenological parameters that characterize the edge structure. The explicit form of the matrix M_τ is determined by the Hermiticity of the Hamiltonian H_τ in a confined region:

$$[M_\tau^\dagger \mathbf{n} \sigma_\tau M_\tau + \mathbf{n} \sigma_\tau]_{\text{edge}} = 0, \quad (3)$$

where $\sigma_\tau = (\tau\sigma_x, \sigma_y)$ is a vector of the Pauli matrix and $\mathbf{n} = (n_x, n_y)$ is an outer unit normal to the edge. Equation (3) can also be obtained from the requirement of a vanishing normal component of the probability current at the edge [22]. Time-reversal symmetry relates the matrices in BC (2) from the two valleys: $M_\tau^{-1} = M_{-\tau}^*$. These conditions lead us to the four-parametric form of matrix M_τ :

$$M_\tau = ie^{i\chi} [\sigma_0 \sinh \xi + \tau \sigma_z \cosh \xi \cosh \eta \cos \nu - i\tau \mathbf{n} \sigma_\tau \cosh \xi (\sinh \eta + \sigma_z \cosh \eta \sin \nu)], \quad (4)$$

where σ_0, σ_z are the identity and third Pauli matrices, respectively, and χ, ξ, η, ν ($0 \leq \chi, \nu < 2\pi$, $-\infty < \xi, \eta < +\infty$) are real phenomenological parameters characterizing edge properties. As matrix M_τ depends on the parameter χ through a common phase factor $e^{i\chi}$ that we assume is constant as a function of the coordinate along the translation-invariant edge, we eliminate it by means of a unitary transformation, $(\tilde{\Psi}_\tau^\uparrow, \tilde{\Psi}_\tau^\downarrow)^T = U(\Psi_\tau^\uparrow, \Psi_\tau^\downarrow)^T$, where $U = \text{diag}\{\sigma_0, e^{-i\chi}\sigma_0\}$. Thus, only three boundary parameters, ξ, η, ν , characterize the translation-invariant edge in the TMD monolayer in the absence of intervalley interaction. Their physical meaning may be obtained by considering limiting cases of the BC (2). In the limit $\xi \rightarrow +\infty$, two-component wave functions with opposite spins become decoupled and satisfy the BC (for a derivation, see Appendix A):

$$[\psi_{c,\tau}^{\uparrow(\downarrow)} - ia_{s,\tau} e^{-i\tau\varphi} \psi_{v,\tau}^{\uparrow(\downarrow)}]_{\text{edge}} = 0, \quad (5)$$

where $a_{s,\tau} = s\tau(1 + s\tau \cosh \eta \cos \nu) / (\sinh \eta + \cosh \eta \sin \nu)$, φ is an angle characterizing the unit normal $\mathbf{n} = (\cos \varphi, \sin \varphi)$, and $s = +1$ (-1) for spin-up (spin-down) states. However, disentanglement of the wave functions belonging to opposite spin projections in BC (5) does not mean vanishing ESOI, as $a_{1,\tau} \neq a_{-1,\tau}$ in the general case. It is known [23] that BC (5) is equivalent to the insertion of a diagonal in the spin subspace potential in the Hamiltonian (1), which is a combination of electrostatic ($\propto \sigma_0$) and pseudoelectrostatic ($\propto \sigma_z$) potentials, $V_{\text{edge}}^{\uparrow(\downarrow)} = [V(\mathbf{r})/2][\sigma_0(1 - a_{s,\tau}^2) + \sigma_z(1 + a_{s,\tau}^2)]$, where $V(\mathbf{r})$ tends to infinity outside the two-dimensional (2D) material and is zero inside of it. The sign of $a_{s,\tau}$ is determined by the sign of $V(\mathbf{r})$ outside of the TMD monolayer. In addition, at $\eta \rightarrow +\infty$ in BC (5), values of the boundary parameters $a_{\pm 1,\tau}$ coincide and equal $a = \cos \nu / (1 + \sin \nu)$, which is determined only by the parameter ν . Therefore, we can conclude that

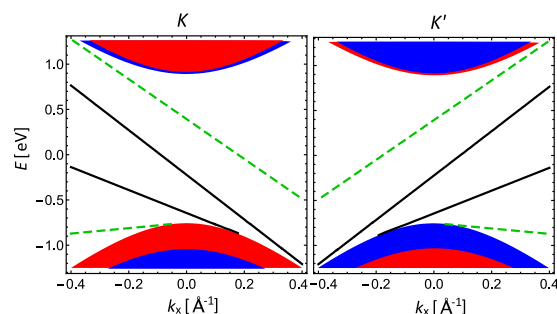


FIG. 1. Solid black and dashed green lines represent typical spectra of ESs in the K (left) and K' (right) valleys derived from Eq. (7) for ESOI described by the following phenomenological parameters: Dashed green lines correspond to $\xi = -2.9$, $\eta = 0.5$, $\nu = 0.6$; solid black lines correspond to $\xi = -2.9$, $\eta = 1.5$, $\nu = 0.6$. Red and blue shaded regions show projections of spin-up and spin-down bulk bands, respectively. Bulk parameters are as follows: $2m = 1.8$ eV, $\Delta_c = 10$ meV, $\Delta_v = 143$ meV, $v = 2.5$ eV Å.

ξ and η describe different types of ESOI, like Rashba and Dresselhaus *interface* spin-orbit parameters for Schrodinger's electrons in GaAs/ $\text{Al}_x\text{Ga}_{1-x}\text{As}$ quantum wells [24], but ν is responsible for coupling bands with the same spin.

Now we are able to calculate spectra of ESs with the general BCs (2) and (4). Suppose that the 2D crystal fills a half plane $y > 0$. Then, the ES wave function has the form

$$\Psi_\tau^{\uparrow(\downarrow)} = C_\tau^{\uparrow(\downarrow)} \begin{pmatrix} 1 \\ \frac{\hbar v(\tau k_x - \kappa_\tau^{\uparrow(\downarrow)})}{\varepsilon + m - s\tau \Delta_v} \end{pmatrix} e^{-\kappa_\tau^{\uparrow(\downarrow)} y + i k_x x}, \quad (6)$$

where $C_\tau^{\uparrow(\downarrow)}$ is a normalization constant and $\kappa_\tau^{\uparrow(\downarrow)} = \{k_x^2 - (\varepsilon - m + s\tau \Delta_c)(\varepsilon + m - s\tau \Delta_v) / (\hbar v)^2\}^{1/2}$ is the decay length of ESs. Substituting wave function (6) in the BC (2), we obtain a general dispersion equation for ESs:

$$\begin{aligned} & \left[1 + a_{+1,\tau} \frac{\hbar v(\tau k_x - \kappa_\tau^\uparrow)}{\varepsilon + m - \tau \Delta_v} \right] \left[1 + a_{-1,\tau} \frac{\hbar v(\tau k_x - \kappa_\tau^\downarrow)}{\varepsilon + m + \tau \Delta_v} \right] \\ & + \frac{\tau v (\tanh \xi - 1)}{\sinh \eta + \cosh \eta \sin \nu} \left[\frac{\hbar v(\tau k_x - \kappa_\tau^\uparrow)}{\varepsilon + m - \tau \Delta_v} - \frac{\hbar v(\tau k_x - \kappa_\tau^\downarrow)}{\varepsilon + m + \tau \Delta_v} \right] \\ & = 0. \end{aligned} \quad (7)$$

In Fig. 1 we reveal the typical dispersion of ESs in the K and K' valleys given by the above equation. In the general case, ESs possess linear dispersion and exist for those longitudinal momenta when their energies do not overlap with projections of bulk bands. The second term on the left-hand side of Eq. (7) is responsible for coupling spins due to ESOI as it goes to zero at $\xi \rightarrow +\infty$, which is the above-discussed limit of spin disentanglement. In this limit, ES spectra are determined by their own parameter $a_{s,\tau}$ for each spin projection:

$$\varepsilon_{e,\tau}^{\uparrow(\downarrow)}(p_x) = -\tau \tilde{v}_{s,\tau} p_x + \varepsilon_{s,\tau}, \quad (8)$$

where $\tilde{v}_{s,\tau} = 2a_{s,\tau} v / (1 + a_{s,\tau}^2)$ is an effective speed of ESs, $\varepsilon_{s,\tau} = \tilde{m}_{s,\tau}(a_{s,\tau}^2 - 1) / (a_{s,\tau}^2 + 1) + s\tau(\Delta_c + \Delta_v)/2$ is the energy of ESs at the center of the corresponding valley, and $\tilde{m}_{s,\tau} = m - s\tau(\Delta_v - \Delta_c)/2$. The valley index τ determines the chirality of ESs (see Fig. 2) which exist for those wave

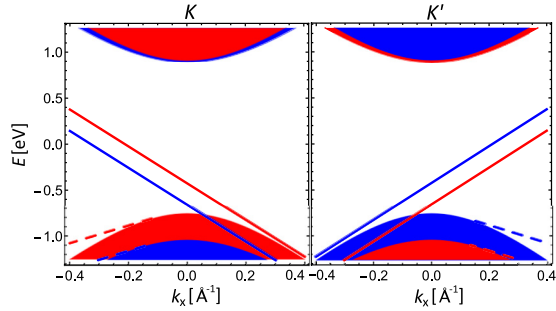


FIG. 2. Red (blue) lines show spectra of spin-up (spin-down) ESs (8) in the K (left) and K' (right) valleys in the absence of ESOI (i.e., $a_{+1,\tau} = a_{-1,\tau}$). Solid lines correspond to $a_{±1,\tau} = 0.5$; dashed lines correspond to $a_{±1,\tau} = -0.2$. Red and blue shaded regions show projections of spin-up and spin-down bulk bands, respectively. Bulk parameters are the same as in Fig. 1.

vectors k_x while their decay length is positive:

$$\kappa_{\tau}^{\uparrow(\downarrow)} = \frac{\tau k_x}{\tilde{m}_{s,\tau}} \left(\varepsilon_{s,\tau} - s\tau \frac{\Delta_v + \Delta_c}{2} \right) + \frac{\tilde{m}_{s,\tau} \tilde{v}_{s,\tau}}{\hbar v^2} > 0. \quad (9)$$

We note that condition (9) allows spin-polarized ESs to exist even when their spectra overlap with the projection of the bulk band characterized by opposite spin. In particular, inequality (9) specifies that at $a_{s,\tau} > 0$ ES spectra intersect the bulk gap, but at $a_{s,\tau} < 0$ they are out of the gap (see Fig. 2). Wave functions of ESs with spectrum (8) read as follows:

$$\Psi_e^{\uparrow(\downarrow)} = C_{\tau}^{\uparrow(\downarrow)} \left(\frac{1}{-a_{s,\tau}} \right) e^{-\kappa_{\tau}^{\uparrow(\downarrow)} y + i k_x x}, \quad (10)$$

where $C_{\tau}^{\uparrow(\downarrow)} = [2a_{s,\tau}^2 \kappa_{\tau}^{\uparrow(\downarrow)} / L_x (1 + a_{s,\tau}^2)]^{1/2}$ is the normalization factor.

Here we point out that in the absence of ESOI ($\xi, \eta \rightarrow +\infty$), ES spectra for two spins are parallel to each other with a constant energy difference for every momentum: $\varepsilon_{e,\tau}^{\uparrow} - \varepsilon_{e,\tau}^{\downarrow} = 2\tau(\Delta_v + a^2 \Delta_c) / (1 + a^2)$.

III. SPIN-VALLEY EDGE PHOTOCURRENTS

In this section we reveal that illumination of a semi-infinite 2D TMD crystal by circularly polarized light induces spin- and valley-polarized edge photocurrents. As we mentioned in the Introduction, the effect is due to the difference in transition probabilities between bulk and edge bands in the two valleys caused by the light.

For definiteness and simplicity we consider the absence of spin-orbit interaction at the edge. Therefore, ESs are described by a single parameter a for both spins and valleys (we suppressed spin and valley indexes). However, the obtained results are also valid when the two spin-polarized ES branches are described by different parameters, $a_{+1,\tau} \neq a_{-1,\tau}$ (8), while one can populate only one of them in each valley. We will assume that $a \sim 1$, so that ES spectra intersect the gap as shown in Fig. 3. This situation agrees with tight-binding calculations of ES spectra at the zigzag edge of MoS₂ [15]. Throughout this section we suppress the valley index τ everywhere except where it is needed.

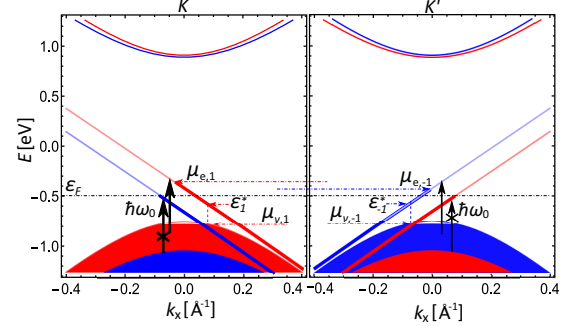


FIG. 3. Schematic picture of quasi-Fermi levels in edge ($\mu_{e,\pm 1}$) and valence ($\mu_{v,\pm 1}$) bands under illumination of clockwise circularly polarized light with frequency ω_0 in the case of spin-polarized ESs described by formula (8) with $a_{+,\tau} = a_{-,\tau} > 0$. ε_F is equilibrium Fermi energy. $\varepsilon_{\pm 1}^*$ is the minimal energy of ESs that radiatively recombine with holes in the valence band.

Now we turn to the bulk states. Below we are interested only in valence band states with energies around the band extremum. In this limit ($vp \ll 2\tilde{m}$) spectra of the spin-up (spin-down) states in the valence band of the K (K') valley are expressed as follows:

$$\varepsilon_v = \varepsilon_t - \frac{(vp)^2}{2\tilde{m}}, \quad (11)$$

where $\varepsilon_t = -m + \Delta_v$ is the energy of the upper valence band top in each valley and $p = \sqrt{p_x^2 + p_y^2}$ is the 2D momentum modulus. Under the assumption about the type of edge mentioned above, bulk states should satisfy the BC (5) with the same parameter a for both spins. This BC is satisfied by a superposition of incident plane wave and plane wave scattered off the edge with a common longitudinal momentum p_x :

$$\Psi_{p_x, \varepsilon_v} = \frac{1}{\sqrt{2}} [\psi_{p_x, -p_y} + R_{\varepsilon_v, k_x} \psi_{p_x, p_y}], \quad (12)$$

where $\psi_{p_x, \pm p_y}$ are plane-wave solutions of the Hamiltonian (1) in the limit $vp \ll 2\tilde{m}$ and R_{ε_v, k_x} is a reflection coefficient that is determined by the BC. Plane-wave states around extremum of the valence band have the form (see Appendix B)

$$\psi_{p_x, p_y} = \frac{1}{\sqrt{L_x L_y}} \begin{pmatrix} -\frac{vp}{2\tilde{m}} \\ e^{i\vartheta_p} \end{pmatrix} e^{i\mathbf{k}\mathbf{r}}, \quad (13)$$

where $L_x L_y$ is the system area, $e^{i\vartheta_p} = p_{+,\tau} / p$, and $\mathbf{k} = (p_x, p_y) / \hbar$ is the 2D wave vector. In fact in the semi-infinite sample p_y is not a good quantum number and should be treated as a function of energy and p_x from Eq. (11): $p_y(\varepsilon, p_x) = [\sqrt{2\tilde{m}/v} \sqrt{\varepsilon_t - \varepsilon_v - (vp_x)^2 / 2\tilde{m}}]$. For valence band states with energies around the band extremum the reflection coefficient can be approximated as follows: $R_{\varepsilon_v, k_x} \approx -e^{-i2\vartheta_p}$.

We suppose that the semi-infinite 2D crystal is illuminated in the negative direction of the z axis by a clockwise polarized light with frequency ω_0 [in the case of counterclockwise polarization one should exchange $\tau \rightarrow -\tau$ in the final formulas (19) and (20)]. Due to spin splitting of the valence bands (on the order of 0.1 eV) one can tune the frequency ω_0 of the illuminated light and Fermi energy ε_F in the monolayer to

induce electrical dipole transitions only from the upper valence band in the K (K') valley to ESs with the corresponding spin (see Fig. 3). Our aim is to calculate the induced edge photocurrent owing to these transitions. To this end we derive a kinetic equation for the distribution function in the framework of the Keldysh formalism [25] (see Appendix C):

$$\begin{aligned} \frac{\partial f_e(\varepsilon)}{\partial t} &= W_{\varepsilon-\hbar\omega_0,\varepsilon}^{\text{ind}} [f_v(\varepsilon - \hbar\omega_0) - f_e(\varepsilon)] \\ &\quad - f_e(\varepsilon) \int_0^{+\infty} W_{\varepsilon-\hbar\omega,\varepsilon}^{\text{sp}} [1 - f_v(\varepsilon - \hbar\omega)] d\omega \\ &\quad - \frac{f_e(\varepsilon) - f_{eq}(\varepsilon)}{\tau_R}, \end{aligned} \quad (14)$$

where $f_{e,v}(\varepsilon)$ are the Fermi-Dirac distribution functions for states in the edge and valence bands, respectively; $f_{eq}(\varepsilon)$ is the equilibrium Fermi-Dirac function; $W_{\varepsilon-\hbar\omega_0,\varepsilon}^{\text{ind}}$ is the rate of induced transitions between ES, characterized by longitudinal momentum p_e and energy ε , and the valence band state with the same longitudinal momentum and energy $\varepsilon - \hbar\omega_0$; $W_{\varepsilon-\hbar\omega,\varepsilon}^{\text{sp}}$ is the rate of spontaneous transitions caused by interaction with the ground state of the electromagnetic field; and τ_R is a phenomenological relaxation time that describes other relaxation processes between edge and valence band states caused by, for example, phonon or electron-electron scattering (below we discuss the range of the relaxation time). The rate of the induced transitions reads as follows:

$$W_{\varepsilon-\hbar\omega_0,\varepsilon}^{\text{ind}} = \frac{2\pi}{\hbar} \frac{I\Omega}{c\hbar\omega_0} |V_{\varepsilon-\hbar\omega_0,\varepsilon}^{(+,\tau)}(\mathbf{q}_0)|^2 \rho_{v,e}(\varepsilon - \hbar\omega_0), \quad (15)$$

where I is the intensity of the incident light, c is the speed of light, Ω is the volume for the quantization of the electromagnetic field, $V_{\varepsilon-\hbar\omega_0,\varepsilon}^{(+,\tau)}(\mathbf{q}_0)$ is the matrix element of the interaction between valence and edge band states (C4), and the density of the valence band states with definite longitudinal momentum p_e near valence band extrema is expressed by the formula

$$\rho_{v,e}(\varepsilon) = \sum_{p_y} \delta(\varepsilon - \varepsilon_{p_e,p_y}) = \frac{L_y \sqrt{2\tilde{m}}}{2\pi \hbar v} \frac{\Theta(\varepsilon_t - \frac{v^2 p_e^2}{2\tilde{m}} - \varepsilon)}{\sqrt{\varepsilon_t - \frac{v^2 p_e^2}{2\tilde{m}} - \varepsilon}}, \quad (16)$$

where $\Theta(\dots)$ is the Heaviside step function. The probability of spontaneous transitions is expressed as follows:

$$W_{\varepsilon-\hbar\omega,\varepsilon}^{\text{sp}} = \frac{\Omega}{(2\pi)^2 \hbar c^3} \sum_{\lambda=\pm} \int d\omega_q |V_{\varepsilon-\hbar\omega,\varepsilon}^{(\lambda,\tau)}(\mathbf{q})|^2 \rho_{v,e}(\varepsilon - \hbar\omega), \quad (17)$$

where integration goes over a solid angle of the light wave vector \mathbf{q} and summation runs over clockwise ($\lambda = +$) and counterclockwise ($\lambda = -$) polarization of the electromagnetic field.

It is known that intraband energy relaxation processes have the shortest times in MoS₂ monolayers [26,27] (on the order of picoseconds). As electron-electron scattering is very efficient in one dimension [28] and also due to the possibility of relaxation in the edge band via scattering by bulk phonons, we suppose that the relaxation time within the edge band is of the same order. This allows us to solve the kinetic

equation (14) in the quasiequilibrium approximation, which is justified when intraband relaxation times are shorter than edge-bulk energy relaxation times. Therefore, we look for a distribution function of the edge (valence) states in the form of the Fermi-Dirac function with its own quasi-Fermi level $\mu_{e,\tau}$ ($\mu_{v,\tau}$). We also suppose that additional edge-to-valence-band energy relaxation processes, characterized by the relaxation time τ_R , are on the order of nanoseconds. This is mainly due to the suppression of phase space for these processes caused by the great difference in the densities of bulk and edge states. This allows edge-to-valence scattering only with certain longitudinal momentum mismatch (as the valence band quasi-Fermi level locates around the top of the valence band).

We are interested in a stationary solution that equates the right-hand side of Eq. (14) to zero. After integrating the kinetic equation over energy in the limit of zero temperature, we arrive at the first implicit relation for $\mu_{e,\tau}$ and $\mu_{v,\tau}$ (D2). Another relation between quasi-Fermi levels is imposed by a particle conservation rule (i.e., the number of holes in the valence band equals the number of photoexcited electrons in the edge band):

$$(\varepsilon_t - \mu_{v,\tau})\rho_v = (\mu_{e,\tau} - \varepsilon_F)\rho_e, \quad (18)$$

where $\rho_v = L_y L_x \tilde{m}/2\pi(\hbar v)^2$ is the density of states in the valence band and $\rho_e = L_x/2\pi\hbar|\tilde{v}|$ is the density of edge states. By virtue of the ratio between the densities $\rho_e/\rho_v \propto \hbar v/\tilde{m}L_y \ll 1$ one has the inequality $|\varepsilon_v - \mu_{v,\tau}| \ll |\mu_{e,\tau} - \varepsilon_F|$, which leads us to a simpler equation for $\mu_{e,\tau}$ [in comparison with Eq. (D2)]:

$$\frac{I}{I_0} \left[\delta_{\tau,1} + \delta_{\tau,-1} \left(\frac{\hbar v \kappa_F}{2\tilde{m}a} \right)^2 \right] G(\mu_{e,\tau} - \hbar\omega_0) - \frac{\mu_{e,\tau} - \varepsilon_F}{\hbar\omega_0^2 \tilde{\tau}_R} = 0, \quad (19)$$

where $I_0 = \hbar\omega_0^4/c^2$, $\tilde{\tau}_R = \tau_R[(v/c)^2(e^2/\hbar c)4\pi a^2/(1+a^2)n_r^2]$ (n_r is the refractive index of the environment), and

$$G(\varepsilon) = \arctan \left(\frac{k_{y0}(\varepsilon)}{\kappa_F} \right) - \frac{\kappa_F k_{y0}(\varepsilon)}{\kappa_F^2 + k_{y0}^2(\varepsilon)},$$

where $k_{y0}(\mu_{e,\tau} - \hbar\omega_0) = p_y(\mu_{e,\tau} - \hbar\omega_0, p_x = 0)/\hbar$. In deriving Eq. (19) we neglected the dependence of the decay length of ESs on the energy [i.e., $\kappa(\varepsilon) \approx \kappa(\varepsilon_F) \equiv \kappa_F$]. We also disregarded the dependence of the momentum component $p_y(\varepsilon, p_e)$ on p_e since we consider the valence band states around the band extremum, i.e., with longitudinal momenta $vp_e \ll 2\tilde{m}$. The expression in the square brackets in Eq. (19) describes the distinction in probabilities of transitions from valence band states (12) to ESs (6) in the K and K' valleys, which significantly differs from selection rules for interband transitions in the bulk [21]. This results in an uncompensated edge photocurrent with a specific spin in a particular valley. In the limit $|\mu_{e,\tau} - \varepsilon_F|/\varepsilon_F \ll 1$ we obtain an explicit expression for the electron quasi-Fermi level in the edge band:

$$\mu_{e,\tau} = \varepsilon_F + \frac{\frac{I}{I_0} \hbar\omega_0^2 \tilde{\tau}_R G(\varepsilon_F - \omega_0) [\delta_{\tau,1} + \delta_{\tau,-1} \left(\frac{\hbar v \kappa_F}{2\tilde{m}a} \right)^2]}{1 - \frac{I}{I_0} \hbar\omega_0^2 \tilde{\tau}_R \frac{\partial G(\varepsilon_F - \omega_0)}{\partial \varepsilon} [\delta_{\tau,1} + \delta_{\tau,-1} \left(\frac{\hbar v \kappa_F}{2\tilde{m}a} \right)^2]}. \quad (20)$$

With known quasi-Fermi levels of the ESs in the two valleys, we use a standard formula for one-dimensional current along

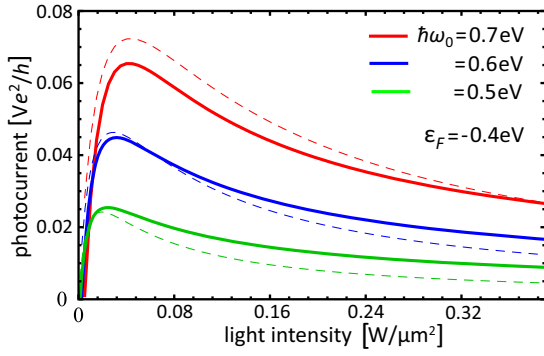


FIG. 4. Dependence of photocurrent (21) on the intensity of illuminating light at three different frequencies: $\hbar\omega_0 = 0.7$ eV (red), $\hbar\omega_0 = 0.6$ eV (blue), and $\hbar\omega_0 = 0.5$ eV (green). Solid lines represent the solution for quasi-Fermi levels derived from Eq. (D2). Dashed lines correspond to the approximated solution (20). The equilibrium Fermi energy is $\varepsilon_F = -0.4$ eV. Bulk parameters are similar to those in Fig. 1, with boundary parameter $a = 0.8$. The phenomenological relaxation time $\tau_R = 1$ ns, and the length characterizing the TMD monolayer perpendicular to the edge direction is $L_y = 1$ μm .

the sample edge:

$$j = \frac{e}{h}(\mu_{e,1} - \mu_{e,-1}). \quad (21)$$

The dependence of the photocurrent on the light intensity is plotted in Fig. 4. Solid lines show the photocurrent obtained by solving Eq. (D2) for electron quasi-Fermi levels; dashed lines represent the approximated solution (20). At low intensities, the current (21) is a linear function of the intensity with a tilt that is determined by the edge-valence-band transition probability difference in the K and K' valleys. However, in the limit of high intensities the current goes to zero as edge bands in both valleys tend to equal the population. This gives rise to a maximum photocurrent in the middle region of intensities. Here we notice that light intensity as high as hundreds of milliwatts per square micrometer in a continuous-wave regime for the near-infrared range of wavelengths can be realized by means of fiber lasers [29]. Using the solutions (20), one can obtain an approximated expression for maximal current in Fig. 4:

$$j_{\max} = \frac{e}{h}(\varepsilon_t - \varepsilon_F + \omega_0) \frac{1 - \left(\frac{\hbar v \kappa_F}{2\tilde{m}a}\right)^2}{1 + \left(\frac{\hbar v \kappa_F}{2\tilde{m}a}\right)^2}, \quad (22)$$

which is valid in the limit $k_{y0}(\varepsilon_F - \omega_0)/\kappa_F \ll 1$. Therefore, the greater edge-valence-band transition probability difference in the two valleys is, the higher the maximal value of spin-valley-polarized current along the edge is. Absolute values of the maximal current can reach several microamperes. In the case of clockwise polarization of light, uncompensated photocurrent flows in the K valley in the negative direction along the edge (see Fig. 3). As mentioned above for counterclockwise polarization, one should exchange $\tau \rightarrow -\tau$ in (20), which leads to uncompensated photocurrent in the K' valley but in the positive direction along the edge. Thus, the direction of light polarization controls not only spin and valley polarization of the uncompensated edge photocurrent but also its flow direction.

IV. CONCLUSION

We developed a theory of ESs in monolayers of TMD crystals which takes into account ESOI within intravalley approximation. The theory relies on a general BC comprising three real phenomenological parameters, ξ, η, ν , that characterize the microscopic structure of the edge. We revealed that ξ is responsible for spin coupling, η accounts for the inequivalence of the edge structure for opposite spin projections in the case of decoupled spins, and ν describes the interband interaction of states with the same spin. In the general case, ESs have linear spectra determined by all three parameters. However, in the case of decoupled spins ($\xi \rightarrow +\infty$), ES spectra become chiral in the valley index and are described by a single parameter (which is a function of η and ν) for each spin projection. The sign of the latter parameter determines whether ES spectra are in the bulk gap or outside of it.

We also considered optical pumping from valence band states to ESs in the absence of the ESOI and demonstrated the possibility for generation of spin- and valley-polarized edge photocurrents. We revealed that the direction and valley and spin polarization of the photocurrent are determined by the direction of circular polarization of the light. Maximal values of the photocurrent are of the order of several microamperes.

ACKNOWLEDGMENT

This work was supported by the Russian Foundation for Basic Research (Project No. 16-32-00655).

APPENDIX A: DERIVATION OF THE SPIN-POLARIZED BC (5)

In the limit $\xi \rightarrow +\infty$ the general BC (2) with matrix M_τ (4) is reduced to the following:

$$\left[\begin{array}{c} \frac{-ie^{-\xi-i\chi}}{1 + \tau \cosh \eta \cos \nu} \begin{pmatrix} 1 & 0 \\ 0 & ia_{1,\tau} e^{-i\tau\varphi} \end{pmatrix} \Psi_\tau^\uparrow \\ + \begin{pmatrix} 1 & -ia_{-1,\tau} e^{-i\tau\varphi} \\ 1 & -ia_{-1,\tau} e^{-i\tau\varphi} \end{pmatrix} \Psi_\tau^\downarrow \end{array} \right]_{\text{edge}} = 0, \quad (A1)$$

where $a_{\pm 1,\tau} = \pm\tau(1 \pm \tau \cosh \eta \cos \nu)/(\sinh \eta + \cosh \eta \sin \nu)$ and we used the identity

$$\frac{\sinh \eta - \cosh \eta \sin \nu}{1 + \tau \cosh \eta \cos \nu} = -\frac{1 - \tau \cosh \eta \cos \nu}{\sinh \eta + \cosh \eta \sin \nu}.$$

In the limit under consideration, wave functions accounting for opposite spin projections are decoupled in the BC, as the coefficient under Ψ_τ^\uparrow in Eq. (A1) is exponentially small. This leads us to a BC for spin-down states:

$$[\psi_c^\downarrow - ia_{-1,\tau} e^{i\tau\varphi} \psi_v^\downarrow]_{\text{edge}} = 0, \quad (A2)$$

where $\Psi_\tau^\downarrow = (\psi_c^\downarrow, \psi_v^\downarrow)$. Subtracting the second row of the BC (A1) from the first one, we arrive at a BC for spin-up states:

$$[\psi_c^\uparrow - ia_{1,\tau} e^{-i\tau\varphi} \psi_v^\uparrow]_{\text{edge}} = 0, \quad (A3)$$

where $\Psi_\tau^\uparrow = (\psi_c^\uparrow, \psi_v^\uparrow)$.

APPENDIX B: APPROXIMATE PLANE-WAVE SOLUTIONS OF THE HAMILTONIAN (1) AROUND BULK BAND EXTREMA

In this appendix we find plane-wave solutions of the Hamiltonian (1) in a system without edge and show that for energies around valence band extrema they are expressed by formula (13). For simplicity we consider only spin-up electrons in the K valley (i.e., $\tau = 1$) and suppress the spin and valley indexes below in this section. Therefore, components $\psi_{1,2}$ of a plane-wave solution $\Psi_{\mathbf{p}} = [e^{i\mathbf{p}\mathbf{r}/\hbar}/(L_x L_y)^{1/2}](\psi_1, \psi_2)^T$ satisfy the system

$$\begin{aligned} (m + \Delta_c - \varepsilon)\psi_1 + v(\tau p_x - i p_y)\psi_2 &= 0, \\ v(\tau p_x + i p_y)\psi_1 + (-m + \Delta_v - \varepsilon)\psi_2 &= 0. \end{aligned} \quad (\text{B1})$$

Together with the normalization condition

$$\int_{-L_x/2}^{L_x/2} dx \int_{-L_y/2}^{L_y/2} dy \Psi_{\mathbf{p}}^* \Psi_{\mathbf{p}} = 1,$$

solutions for the amplitudes can be represented as follows:

$$\begin{aligned} \psi_1 &= \frac{(\varepsilon_{c,v} + m - \Delta_v)}{[(\varepsilon_{c,v} + m - \Delta_v)^2 + (vp)^2]^{1/2}}, \\ \psi_2 &= \frac{vpe^{i\theta_p}}{[(\varepsilon_{c,v} + m - \Delta_v)^2 + (vp)^2]^{1/2}}, \end{aligned} \quad (\text{B2})$$

where energies for the plane-wave solutions read as follows:

$$\varepsilon_{c,v} = (\Delta_v + \Delta_c)/2 \pm \sqrt{\tilde{m}^2 + (vp)^2}, \quad (\text{B3})$$

where the plus (minus) sign before the square root corresponds to bulk states in the conduction (valence) band. Finally, expanding energies of the valence band states (B3) in expressions for the amplitudes (B2) around the band extremum (i.e., at $vp \ll 2\tilde{m}$), $\varepsilon_v \approx -m + \Delta_v + (vp)^2/2\tilde{m}$, we obtain the following expression for the plane-wave solutions in the vicinity of the valence band maximum:

$$\Psi_{\mathbf{p}} = \frac{1}{\sqrt{L_x L_y}} \begin{pmatrix} -\frac{vp}{2\tilde{m}} \\ e^{i\theta_p} \end{pmatrix} e^{i\mathbf{p}\mathbf{r}/\hbar}, \quad (\text{B4})$$

which is identical to Eq. (13) in the main text. For the states around the conduction band minimum $\varepsilon_c \approx m + \Delta_c + (vp)^2/2\tilde{m}$, one can obtain the following expression:

$$\Psi_{\mathbf{p}} = \frac{1}{\sqrt{L_x L_y}} \begin{pmatrix} 1 \\ \frac{vp}{2\tilde{m}} e^{i\theta_p} \end{pmatrix} e^{i\mathbf{p}\mathbf{r}/\hbar}. \quad (\text{B5})$$

APPENDIX C: DERIVATION OF THE KINETIC EQUATION (14)

In order to derive the kinetic equation (14) we first write down the Hamiltonian of the system under consideration in terms of second-quantization operators:

$$\begin{aligned} H_0 &= \sum_{p_e} \varepsilon_e a_{p_e}^+ a_{p_e} + \sum_{p_x, p_y} \varepsilon_{v, p_x, p_y} a_{v, p_x, p_y}^+ a_{v, p_x, p_y} \\ &+ \sum_{p_x, p_y} \varepsilon_{c, p_x, p_y} a_{c, p_x, p_y}^+ a_{c, p_x, p_y} \\ &+ \sum_{\mathbf{q}, \lambda = \pm} \hbar\omega \left(c_{\mathbf{q}, \lambda}^+ c_{\mathbf{q}, \lambda} + \frac{1}{2} \right), \end{aligned} \quad (\text{C1})$$

where a_{p_e} ($a_{p_e}^+$) is the annihilation (creation) operator of the edge state (10) with energy ε_e , $a_{v/c, p_x, p_y}$ ($a_{v/c, p_x, p_y}^+$) is the annihilation (creation) operator of the valence/conduction band state (12) with energy $\varepsilon_{v/c, p_x, p_y}$, $c_{\mathbf{q}, \lambda}$ ($c_{\mathbf{q}, \lambda}^+$) is the annihilation (creation) operator of a photon with clockwise ($\lambda = +$) or counterclockwise ($\lambda = -$) polarization, and energy $\omega = cq$. In the above equation we suppress spin and valley indexes for brevity. In terms of the creation and annihilation operators of a photon field the vector potential reads as follows:

$$\mathbf{A}(\mathbf{r}, t) = \sum_{\mathbf{q}, \lambda = \pm} \sqrt{\frac{2\pi c^2 \hbar}{n_r^2 \omega \Omega}} [c_{\mathbf{q}, \lambda} \mathbf{e}_{\mathbf{q}, \lambda} e^{i(\mathbf{q}\mathbf{r} - \omega t)} + c_{\mathbf{q}, \lambda}^+ \mathbf{e}_{\mathbf{q}, \lambda}^* e^{-i(\mathbf{q}\mathbf{r} - \omega t)}], \quad (\text{C2})$$

where Ω is the quantization volume and polarization unit vectors $\mathbf{e}_{\mathbf{q}, \pm} = [1/\sqrt{2}](\cos \alpha_q \pm i \sin \alpha_q \cos \theta_q, -\sin \alpha_q \pm i \cos \alpha_q \cos \theta_q, \mp i \sin \theta_q)$ [spherical angles α_q, θ_q characterize the direction of the photon wave vector $\mathbf{q} = q(\sin \alpha_q \sin \theta_q, \cos \alpha_q \sin \theta_q, \cos \theta_q)$]. The interaction of electrons with the electromagnetic field reads as follows:

$$V_{\text{int}} = \sum_{p_e, p_x, p_y, \mathbf{q}, \lambda = \pm} [V_{\varepsilon_v, \varepsilon_e}^{(\lambda, \tau)}(\mathbf{q}) a_{p_e}^+ c_{\mathbf{q}, \lambda} a_{v, p_x, p_y} + \text{H.c.}], \quad (\text{C3})$$

where we take into account only transitions between valence band electrons and edge states that are determined in the dipole approximation by the matrix elements:

$$\begin{aligned} V_{\varepsilon_v, \varepsilon_e}^{(\lambda, \tau)}(\mathbf{q}) &= \tau \delta_{p_e, p_x} \frac{ve}{c} \sqrt{\frac{2\pi c^2 \hbar}{n_r^2 \omega \Omega}} \frac{C_e \sqrt{L_x}}{\sqrt{2L_y}} \frac{2ik_y(\varepsilon, p_e)}{\kappa^2 + k_y^2(\varepsilon, p_e)} \\ &\times \left[\frac{e^{-i\tau\alpha_q}}{\sqrt{2}} (1 + \tau\lambda \cos \theta_q) \right. \\ &\left. + \frac{e^{i\tau\alpha_q}}{\sqrt{2}} (1 - \tau\lambda \cos \theta_q) \frac{\hbar v \kappa + \tau v p_e}{2\tilde{m}a} \right]. \end{aligned} \quad (\text{C4})$$

From the above formula it follows that the ratio of probabilities for induced transitions (at normal incidence of light $\cos \theta_q = 1$) in the two valleys for definite polarization has an order of $(\hbar v \kappa / 2\tilde{m}a)^2 \approx 1/4 \ll 1$ at the boundary parameter values $|a| \approx 1$.

Now we introduce the Keldysh Green's functions of electrons, $G_v^{\alpha\beta}(t, t') = -i \langle T_C \{ a_v(t^\alpha) a_v^+(t'^\beta) \} \rangle$ (v are quantum numbers of the edge or bulk state), and photons, $D_{\mathbf{q}, \lambda}^{\alpha\beta}(t, t') = -i \langle T_C \{ c_{\mathbf{q}, \lambda}(t^\alpha) c_{\mathbf{q}, \lambda}^+(t'^\beta) \} \rangle$ ($\alpha, \beta = \pm$). Following standard procedure [25], we obtain a kinetic equation for the Green's function that determines the population distribution of edge state [$G_e^<(t, t) = G_e^+(t, t)$]:

$$\begin{aligned} i \frac{\partial}{\partial t} G_e^<(t, t) &= \int_{-\infty}^{+\infty} \Sigma_{ee}^R(t, t_1) G_e^<(t_1, t) dt_1 + \int_{-\infty}^{+\infty} \Sigma_{ee}^<(t, t_1) G_e^A(t_1, t) dt_1 \\ &- \int_{-\infty}^{+\infty} G_e^R(t, t_1) \Sigma_{ee}^<(t_1, t) dt_1 - \int_{-\infty}^{+\infty} G_e^<(t, t_1) \Sigma_{ee}^A(t_1, t) dt_1, \end{aligned} \quad (\text{C5})$$

where $G^R = G^{--} - G^{+-}$ and $G^A = G^{--} - G^{+-}$. In Eq. (C5) we calculate self-energies in the second order in perturbation (C3):

$$\begin{aligned}
\Sigma_{ee}^R(t_1, t_2) &= \Sigma_{ee}^{--}(t_1, t_2) + \Sigma_{ee}^{-+}(t_1, t_2) \\
&= i \sum_{\mathbf{p}, \mathbf{q}, \lambda} |V_{\varepsilon_v, \varepsilon_e}^{(\lambda, \tau)}(\mathbf{q})|^2 [D_{0\mathbf{q}, \lambda}^{--}(t_1, t_2) G_{0\mathbf{p}, \varepsilon_v}^{--}(t_1, t_2) \\
&\quad - D_{0\mathbf{q}, \lambda}^{-+}(t_1, t_2) G_{0\mathbf{p}, \varepsilon_v}^{-+}(t_1, t_2)] \\
&= -i\theta(t_1 - t_2) \\
&\quad \times \sum_{\mathbf{p}, \mathbf{q}, \lambda} |V_{\varepsilon_v, \varepsilon_e}^{(\lambda, \tau)}(\mathbf{q})|^2 [n_0 \delta_{\lambda, +} \delta_{\mathbf{q}, \mathbf{q}_0} + (1 - f_v)] \\
&\quad \times e^{-i(\varepsilon_v + \omega)(t_1 - t_2)}, \\
\Sigma_{ee}^<(t_1, t_2) &= -\Sigma_{ee}^{-+}(t_1, t_2) \\
&= i \sum_{\mathbf{p}} |V_{\varepsilon_v, \varepsilon_e}^{(+, \tau)}(\mathbf{q}_0)|^2 n_0 f_v e^{-i(\varepsilon_v + \omega)(t_1 - t_2)}, \\
\Sigma_{ee}^R(t_1, t_2) &= [\Sigma_{ee}^A(t_2, t_1)]^*, \tag{C6}
\end{aligned}$$

where the terms with wave vector $\mathbf{q}_0 = (0, 0, -q_0)$ describe transitions induced by illuminated light with frequency $\omega_0 = cq_0$ and clockwise polarization, $n_0 = -iD_{0\mathbf{q}_0, +}^{++}(t, t)$ is the number of the illuminated light quanta, and the term proportional to $1 - f_v$ [where $f_v = -iG_{0\mathbf{p}, \varepsilon_v}^{--}(t, t)$ is the Fermi-Dirac distribution function in the valence band] concerns spontaneous recombination processes. After substituting Green's functions of the zero approximation $G_e^A(t_1, t_2) = [G_e^R(t_2, t_1)]^* = i\theta(t_2 - t_1)e^{i\varepsilon_e(t_2 - t_1)}$, $G_e^<(t_1, t_2) = if_e(t)e^{i\varepsilon_e(t_2 - t_1)}$ in Eq. (C5) and accounting for only contributions from poles at integration, over time we arrive at a kinetic equation similar to that used in the main text [Eq. (14)]:

$$\begin{aligned}
\frac{\partial f_e}{\partial t} &= \frac{I\Omega}{c\hbar\omega_0} \frac{2\pi}{\hbar} \sum_{\mathbf{p}} |V_{\varepsilon_v, \varepsilon_e}^{(+, \tau)}(\mathbf{q}_0)|^2 [f_v - f_e] \delta(\varepsilon_v - \varepsilon_e + \hbar\omega_0) \\
&\quad - f_e \frac{2\pi}{\hbar} \sum_{\mathbf{p}, \mathbf{q}, \lambda = \pm} |V_{\varepsilon_v, \varepsilon_e}^{(\lambda, \tau)}(\mathbf{q})|^2 [1 - f_v] \delta(\varepsilon_v - \varepsilon_e + \hbar\omega) \\
&\quad - \frac{f_e - f_{eq}}{\tau_R}, \tag{C7}
\end{aligned}$$

where we add the term with phenomenological relaxation time τ_R as in the main text, $n_0 = I\Omega/c\hbar\omega_0$.

APPENDIX D: GENERAL RELATION FOR QUASI-FERMI LEVELS

In this Appendix we obtain a general relation for quasi-Fermi levels of electrons in valence and edge bands under illumination of the light. Introducing the density of valence band states with definite momentum (16), we rewrite Eq. (C7) in the following form:

$$\begin{aligned}
\frac{I}{I_0} \left[\delta_{\tau, 1} + \delta_{\tau, -1} \left(\frac{\hbar v \kappa_e + \tau v p_e}{2\tilde{m}a} \right)^2 \right] [f_v(\varepsilon - \hbar\omega_0) - f_e(\varepsilon)] \frac{\sqrt{\varepsilon_t - \frac{v^2 p_e^2}{2\tilde{m}} - \varepsilon + \hbar\omega_0}}{\left[\frac{(\hbar v \kappa_e)^2}{2\tilde{m}} + \varepsilon_t - \frac{v^2 p_e^2}{2\tilde{m}} - \varepsilon + \hbar\omega_0 \right]^2} \\
- \frac{f_e(\varepsilon)}{12\pi^2 (\hbar\omega_0)^2} \left[1 + \left(\frac{\hbar v \kappa_e + \tau v p_e}{2\tilde{m}a} \right)^2 \right] \int_0^{+\infty} d(\hbar\omega) \frac{\hbar\omega [1 - f_v(\varepsilon - \hbar\omega)] \sqrt{\varepsilon_t - \frac{v^2 p_e^2}{2\tilde{m}} - \varepsilon + \hbar\omega}}{\left[\frac{(\hbar v \kappa_e)^2}{2\tilde{m}} + \varepsilon_t - \frac{v^2 p_e^2}{2\tilde{m}} - \varepsilon + \hbar\omega \right]^2} \\
- \frac{(1 + a^2)n_r^2 c^3 \sqrt{2\tilde{m}}}{4a^2 \pi \tau_R (ve)^2 \omega_0^2 \hbar v \kappa_e} [f_e(\varepsilon) - f_{eq}(\varepsilon)] = 0. \tag{D1}
\end{aligned}$$

To proceed further analytically, we consider the low-temperature limit [$T \ll \min(|\mu_{e, \tau} - \varepsilon_F|, |\mu_{v, \tau} - \varepsilon_t|)$] to treat Fermi functions as steplike ones. Then we integrate the above equation over energy and arrive at a final relation between quasi-Fermi levels $\mu_{e, \tau}, \mu_{v, \tau}$:

$$\begin{aligned}
\frac{I}{I_0} \left[\delta_{\tau, 1} + \delta_{\tau, -1} \left(\frac{\hbar v \kappa_F}{2\tilde{m}a} \right)^2 \right] \left\{ \arctan \left[\frac{\kappa_F [k_{y0}(\mu_{e, \tau} - \hbar\omega_0) - k_{y0}(\mu_{v, \tau})]}{\kappa_F^2 + k_{y0}(\mu_{e, \tau} - \hbar\omega_0) k_{y0}(\mu_{v, \tau})} \right] + \frac{\kappa_F k_{y0}(\mu_{v, \tau})}{\kappa_F^2 + k_{y0}^2(\mu_{v, \tau})} \right\} \\
- \theta(\mu_{e, \tau} - \varepsilon^*) \frac{\kappa_F \left[1 + \left(\frac{\hbar v \kappa_0}{2\tilde{m}a} \right)^2 \right]}{12\pi^2 \kappa_0 (\hbar\omega_0)^2} \left\{ 6(\hbar v)^2 \kappa_0 k_{y0}(\mu_{v, \tau}) \frac{\mu_{e, \tau} - \varepsilon^*}{2\tilde{m}} - \frac{\kappa_F k_{y0}(\mu_{v, \tau})}{\kappa_F^2 + k_{y0}^2(\mu_{v, \tau})} [(\mu_{e, \tau} - \mu_{v, \tau})^2 - (\varepsilon^* - \mu_{v, \tau})^2] \right\} \\
+ \arctan \left(\frac{k_{y0}(\mu_{v, \tau})}{\kappa_0} \right) \left[\left(\mu_{e, \tau} - \varepsilon_t - 3 \frac{(\hbar v \kappa_0)^2}{2\tilde{m}} \right)^2 - \left(\varepsilon^* - \varepsilon_t - 3 \frac{(\hbar v \kappa_0)^2}{2\tilde{m}} \right)^2 \right] - \frac{(1 + a^2)n_r^2 c^3}{4a^2 \pi \tau_R \omega_0^2 (ve)^2} [\mu_{e, \tau} - \varepsilon_F] = 0, \tag{D2}
\end{aligned}$$

where $k_{y0}(\varepsilon) = k_y(\varepsilon, 0)$, $\kappa_F = \kappa(\varepsilon_F)$, and $\kappa_0 = \kappa(\varepsilon_e(0))$. At integration we neglected the dependence of ES decay length and terms proportional to $vp_e/2\tilde{m}$ on the energy. In the limit $\rho_e/\rho_v \ll 1$ we can neglect the terms proportional to $k_{y0}(\mu_{v, \tau})$ in Eq. (D2), which leads us to Eq. (19) in the main text.

[1] Z. Sun, A. Martinez, and F. Wang, *Nat. Photonics* **10**, 227 (2016).

[2] A. Pospischil, M. M. Furchi, and T. Mueller, *Nat. Nanotechnol.* **9**, 257 (2014).

- [3] A. Kormányos, G. Burkard, M. Gmitra, J. Fabian, V. Zólyomi, N. D. Drummond, and V. Fal'ko, *2D Mater.* **2**, 022001 (2015).
- [4] G. Moody, C. K. Dass, K. Hao, C.-H. Chen, L.-J. Li, A. Singh, K. Tran, G. Clark, X. Xu, G. Berghäuser *et al.*, *Nat. Commun.* **6**, 8315 (2015).
- [5] X. Yin, Z. Ye, D. A. Chenet, Y. Ye, K. O'Brien, J. C. Hone, and X. Zhang, *Science* **344**, 488 (2014).
- [6] C. Zhang, A. Johnson, C.-L. Hsu, L.-J. Li, and C.-K. Shih, *Nano Lett.* **14**, 2443 (2014).
- [7] M. V. Bollinger, J. V. Lauritsen, K. W. Jacobsen, J. K. Nørskov, S. Helveg, and F. Besenbacher, *Phys. Rev. Lett.* **87**, 196803 (2001).
- [8] D. Wu, X. Li, L. Luan, X. Wu, W. Li, M. N. Yogeesh, R. Ghosh, Z. Chu, D. Akinwande, Q. Niu, and K. Lai, *Proc. Natl. Acad. Sci. USA* **113**, 8583 (2016).
- [9] M. V. Bollinger, K. W. Jacobsen, and J. K. Nørskov, *Phys. Rev. B* **67**, 085410 (2003).
- [10] C. Ataca, H. Sahin, E. Akturk, and S. Ciraci, *J. Phys. Chem. C* **115**, 3934 (2011).
- [11] E. Erdogan, I. Popov, A. Enyashin, and G. Seifert, *Eur. Phys. J. B* **85**, 1 (2012).
- [12] A. Vojvodic, B. Hinnemann, and J. K. Nørskov, *Phys. Rev. B* **80**, 125416 (2009).
- [13] Y. Li, Z. Zhou, S. Zhang, and Z. Chen, *J. Am. Chem. Soc.* **130**, 16739 (2008).
- [14] F. Khoeini, Kh. Shakouri, and F. M. Peeters, *Phys. Rev. B* **94**, 125412 (2016).
- [15] H. Rostami, R. Asgari, and F. Guinea, *J. Phys. Condens. Matter* **28**, 495001 (2016).
- [16] C. G. Péterfalvi, A. Kormányos, and G. Burkard, *Phys. Rev. B* **92**, 245443 (2015).
- [17] V. A. Volkov and V. V. Enaldiev, *J. Exp. Theor. Phys.* **122**, 608 (2016).
- [18] C. Segarra, J. Planelles, and S. E. Ulloa, *Phys. Rev. B* **93**, 085312 (2016).
- [19] M. Trushin, E. J. R. Kelleher, and T. Hasan, *Phys. Rev. B* **94**, 155301 (2016).
- [20] K. F. Mak, K. L. McGill, J. Park, and P. L. McEuen, *Science* **344**, 1489 (2014).
- [21] D. Xiao, G.-B. Liu, W. Feng, X. Xu, and W. Yao, *Phys. Rev. Lett.* **108**, 196802 (2012).
- [22] A. R. Akhmerov and C. W. J. Beenakker, *Phys. Rev. B* **77**, 085423 (2008).
- [23] I. V. Zagorodnev, Z. A. Devizorova, and V. V. Enaldiev, *Phys. Rev. B* **92**, 195413 (2015).
- [24] Z. A. Devizorova, A. V. Shchepetilnikov, Y. A. Nefyodov, V. A. Volkov, and I. V. Kukushkin, *JETP Lett.* **100**, 102 (2014).
- [25] P. I. Arseev, *Phys. Usp.* **58**, 1159 (2015).
- [26] H. Shi, R. Yan, S. Bertolazzi, J. Brivio, B. Gao, A. Kis, D. Jena, H. G. Xing, and L. Huang, *ACS Nano* **7**, 1072 (2013).
- [27] R. Wang, B. A. Ruzicka, N. Kumar, M. Z. Bellus, H.-Y. Chiu, and H. Zhao, *Phys. Rev. B* **86**, 045406 (2012).
- [28] M. Hirtshulz, F. Milde, E. Malic, C. Thomsen, S. Reich, and A. Knorr, *Phys. Status Solidi B* **245**, 2164 (2008).
- [29] V. V. Ter-Mikirtychev, *Fundamentals of Fiber Lasers and Fiber Amplifiers* (Springer, Berlin, 2014).